AJNR

Various Patterns of Perfusion-Weighted MR Imaging and MR Angiographic Findings in Hyperacute Ischemic Stroke

Jae Hyoung Kim, Taemin Shin, Ji Hoon Park, Sung Hoon Chung, Nack-Cheon Choi and Byeong Hoon Lim

AJNR Am J Neuroradiol 1999, 20 (4) 613-620
http://www.ajnr.org/content/20/4/613

AJNR Am J Neuroradiol 20:613–620, April 1999

Various Patterns of Perfusion-Weighted MR Imaging and MR Angiographic Findings in Hyperacute Ischemic Stroke

Jae Hyoung Kim, Taemin Shin, Ji Hoon Park, Sung Hoon Chung, Nack-Cheon Choi, and Byeong Hoon Lim

BACKGROUND AND PURPOSE: **Various clinical subtypes of patients presenting with sudden-onset ischemic stroke have been recognized, but classification of those types is not simple. We identified various patterns of perfusion-weighted MR imaging and MR angiographic findings in hyperacute ischemic stroke with relation to clinical outcomes.**

METHODS: **Twelve patients with symptoms of acute ischemic stroke due to middle cerebral artery occlusion underwent perfusion-weighted MR imaging and MR angiography within 6 hours after the onset of symptoms. Perfusion-weighted imaging was performed with a conventional dynamic contrast-enhanced T2*-weighted sequence, and cerebral blood volume (CBV) maps were then created. CBV maps and MR angiographic findings were compared with ^{99m}Tc-HMPAO brain SPECT scans, short-term outcomes, and follow-up imaging findings.**

RESULTS: **The combined CBV and MR angiographic findings were classified into three patterns: arterial occlusion and decreased CBV (n = 8), arterial occlusion and increased CBV (n = 2), and no arterial occlusion and normal CBV (n = 2). These three patterns were strongly related to SPECT findings, short-term outcomes, and follow-up imaging findings. Perfusion on SPECT decreased markedly in the affected regions in all patients with the first pattern, decreased slightly in the second pattern, and was normal in the third pattern. Symptoms were not significantly changed at 24 hours after onset in any of the patients with the first pattern, but resolved completely in all patients with the latter two patterns. Follow-up imaging showed large infarctions in all patients with the first pattern. Initially, no infarction was seen in the second pattern, but watershed infarction developed later in one of these patients.**

CONCLUSION: **Hyperacute ischemic stroke may be differentiated into three imaging patterns with different clinical outcomes. The combined use of perfusion-weighted MR imaging and MR angiography may play a substantial role in guiding the choice of treatment of this disease.**

Various clinical subtypes of patients who present with sudden onset of symptoms and signs of ischemic stroke have been recognized, but classification of those types is not simple (1). Early diagnosis of acute ischemic stroke has become increasingly important, because aggressive thrombolytic therapy, such as urokinase or tissue plasminogen activator infusion, within the first few hours after the onset of symptoms is effective in improving stroke outcome for a defined subtype of ischemic stroke (2–5). Therefore, it is important to differentiate between those patients with hyperacute ischemic stroke who will benefit from thrombolytic therapy and those who may need other types of treatment. However, comprehensive determination of the origin and pathophysiology of an individual stroke is not easy during the limited therapeutic window that is available.

Recently, promising MR imaging techniques, such as diffusion-weighted and perfusion-weighted imaging, have been applied to patients with acute ischemic stroke for detection of early changes. Although these imaging techniques have become incorporated into imaging protocols for hyperacute ischemic stroke to depict potentially salvageable ischemic tissue (6–8), they are not widely available on current diagnostic MR imaging systems. Unlike diffusion-weighted MR imaging, perfusion-weight-

Received June 11, 1998; accepted after revision November 18.

From the Gyeongsang Institute for Neuroscience (J.H.K., T.S., S.H.C., N.C.C., B.H.L.) and the Research Institute of Industrial Technology (T.S.), Gyeongsang National University; and the Department of Radiology, Gyeongsang National University Hospital (J.H.K., J.H.P., S.H.C.), Chinju, South Korea.

Address reprint requests to Jae Hyoung Kim, MD, Department of Radiology, Gyeongsang National University Hospital, 90 Chilam-dong, Chinju 660–702, South Korea.

ed imaging can easily be performed to evaluate cerebral blood volume (CBV) on a conventional MR imaging system not equipped with strong and fast gradients, and adds only a few minutes to the examination time (9, 10). The region of decreased CBV in hyperacute ischemic stroke has been reported to correspond to the final extent of infarction (11, 12), although, as yet, no consensus exists as to the best hemodynamic parameter that can be measured with perfusion-weighted MR imaging.

We recently observed different patterns of CBV and angiographic findings on MR images of patients with hyperacute ischemic stroke who had been initially considered candidates for our thrombolytic therapy protocol. We hypothesized that different patterns of CBV and MR angiographic findings would reflect different hemodynamic status, and, therefore, would relate to different clinical outcomes. In this study, we performed both perfusion-weighted MR imaging and MR angiography on a conventional MR imaging system in patients with hyperacute ischemic stroke and compared these findings with brain single-photon emission CT (SPECT) scans, short-term clinical outcome, and follow-up imaging findings.

Methods

Patients

A total of 109 consecutive patients with acute ischemic stroke were referred to our hospital during a period of 1 year. Among these, 12 patients with symptoms of middle cerebral artery (MCA) occlusion who underwent MR imaging from 2 to 6 hours (mean, 4.3 hours) after the onset of symptoms as part of our acute stroke protocol were included in this study. Informed consent for this MR examination was obtained from the patients or their family. An initial CT scan was obtained in all patients before MR examination. ^{99m}Tc-HMPAO brain SPECT was performed in nine of 12 patients with injection of tracer within 30 minutes before or after MR imaging.

The seven men and five women in the study were 45 to 81 years old (mean age, 61 years). Nine patients underwent conservative treatment, with or without intravenous heparin therapy, during the acute stage of stroke. Intraarterial urokinase infusion therapy was administered in three patients in accordance with our entry criteria for thrombolytic therapy; however, it failed to effect recanalization of the vascular obstruction in all three patients.

Neurologic Assessment

As a measure of the severity of neurologic deficit, the National Institutes of Health (NIH) Stroke Scale was administered by a neurologist during the hyperacute stage and again 24 hours after symptom onset.

Imaging Studies

MR examinations were performed on a 1.5-T system in accordance with our acute stroke protocol, which consisted of turbo spin-echo T2-weighted imaging, axial spin-echo T1-weighted imaging, MR angiography, and dynamic contrast-enhanced T2*-weighted imaging for perfusion-weighted imaging, and postcontrast T1-weighted imaging, in sequence. The imaging parameters were 3500/90 (TR/TE) for the T2-weighted sequences and 550/14 for the T1-weighted sequences. Section thickness was 5 to 6 mm, and the matrix was 192 × 256. MR angiography was performed around the circle of Willis with a standard 3D time-of-flight sequence (38/7, 15° flip angle, 64-mm slab thickness, and 192 × 256 matrix). Total imaging and processing time was approximately 19 minutes. The total scan time, including the transfer of patients to and from the table, patient positioning, and coil tuning, was less than 25 minutes.

Dynamic contrast-enhanced T2*-weighted imaging was performed with a conventional gradient-echo sequence (40/26, 10° flip angle, 64 × 128 matrix, 5- to 6-mm section thickness, 3.8-second acquisition time). Seventeen single-section dynamic images were obtained at the level of the basal ganglia, which is where the largest infarction is usually detected on T2-weighted images. After acquisition of three images, gadodiamide was administered via the forearm vein as a bolus within 5 seconds, followed by a flush of 30 mL of saline. Total imaging time was approximately 60 seconds after initiation of the bolus injection.

A Siemens Multi-SPECT3 (Chicago, IL) was used for cerebral blood flow (CBF) imaging. Patients received 28 to 35 mCi (1036–1295 MBq) of ^{99m}Tc-HMPAO within 30 minutes before or after MR imaging. Scanning (average acquisition time, 25 minutes) was performed within 6 hours after tracer injection, depending on the patient's condition. Images were reconstructed in a 128 × 128 matrix (9.4 × 9.7-mm in-plane resolution) with 5-mm section thickness in transverse, sagittal, and coronal planes using Butterworth filtered back projection.

Follow-up examinations were performed with CT or MR imaging in 10 patients from 1 to 28 days (mean, 10 days) after the onset of symptoms. An abnormally hypodense area on CT scans or a hyperintense area on T2-weighted images was considered to be the eventual infarction.

Data Analysis

All dynamic MR images were transferred via Ethernet to a personal computer immediately after image acquisition and were evaluated with proprietary software. The CBV maps were created on a pixel-by-pixel basis, assuming an exponential relationship between the relative signal reduction and the contrast material concentration, by numerical integration of the time-concentration curve, similar to that described previously (13). Lesion-to-contralateral CBV ratios were then calculated by placing an irregular but mirror-shaped region of interest (ROI) in the decreased CBV area and in the corresponding contralateral normal area on the CBV maps. When no perfusion abnormality was seen on the CBV maps, the areas of both MCAs were included in the ROIs. We also plotted the time–signal intensity curves in the same regions as above during the bolus passage of the contrast material on the dynamic MR images for side-by-side comparison: signal reduction, arrival time (ie, time to peak signal reduction), and washout pattern of the contrast material were visually compared between hemispheres.

For the analysis of SPECT images, we selected three consecutive transverse images that included the imaging plane of the perfusion-weighted MR study. Symmetrical mirror ROIs were placed on the selected SPECT scans, as in the measurement of the CBV ratios, and lesion-to-contralateral CBF ratios were calculated. The CBF ratios of three sections were then averaged.

Finally, to classify the different imaging patterns of CBV and MR angiographic findings in hyperacute ischemic stroke, we evaluated the CBV changes on perfusion-weighted MR images and the presence or absence of arterial occlusion on MR angiograms. After classifying the imaging patterns, we compared the CBV ratios on perfusion-weighted MR images, the CBF ratios on SPECT scans, and the development of infarction on follow-up images for the different patterns. Patients' short-term outcomes were also evaluated by comparing the NIH Stroke Scale scores in the hyperacute stage and 24 hours after symptom onset with each imaging pattern. We used the Krus-

Summary of findings

Case	Age (y)/ Sex	Initial NIH SS Score and Major Symptoms	Time (h) to Initial MR	Occlusion Site on MR Angiogram	CBV Ratio on Perfusion-Weighted Image	CBF Ratio on SPECT	NIH SS Score at 24 h after Onset	Time (d) to Follow-up Imaging	Site of Final Infarct
1	45/M	17; R hemiparesis, aphasia	5	L M1	0.19	· · ·	17	10	L MCA
2	55/F	22; L hemiparesis	3	R M1	0.03	· · ·	21	7	R MCA
3	55/M	25; R hemiparesis, aphasia	4	L ICA to M1	0.31	0.30	25	1	L MCA
4	49/F	17; L heimparesis	6	R M1	0.21	0.44	16	22	R MCA
5	65/M	27; R hemiparesis, aphasia	4	L ICA to M1	0.08	0.20	27	28	L MCA
6	81/F	14; L hemiparesis	5	R M1	0.36	0.65	9	11	R MCA
7	49/M	12; L hemiparesis	4	R ICA to M1	0.15	0.51	11	3	R MCA
8	77/F	17; L hemiparesis	5	R M1	0.17	0.22	20	3	R MCA
9	67/M	4; R hemiparesis, dysarthria	4	L ICA to M1	1.17	0.89	0	9	Normal*
10	61/M	5; R hemiparesis	6	L ICA to M1	1.23	0.81	0	2	Normal
11	79/F	22; R hemiparesis, aphasia	2	Normal	0.98	· · ·	0	· · ·	· · ·
12	51/M	7; L hemiparesis	3	Normal	1.01	0.99	0	· · ·	· · ·

Note.—ICA indicates internal carotid artery; MCA, middle cerebral artery; M1, M1 segment of MCA; NIH SS, National Institutes of Health Stroke Scale.

* Watershed infarctions developed 12 days after the onset of symptoms.

kal-Wallis test to examine the significance of differences in CBV and CBF ratios, and Fisher's exact test to assess the development of infarction on follow-up images. Wilcoxon matched-pairs signed rank test was used to assess the significance of the short-term interval changes in the NIH Stroke Scale scores. The level of significance of all statistics was defined as $P < .05$. Computations were performed with the SPSS statistical software package (SPSS, Chicago, IL).

Results

The overall results of clinical and imaging findings are summarized in the Table. Five of 12 patients had underlying cardiac problems: acute myocardial infarction with atrial fibrillation (case 2), dilated cardiomyopathy with atrial fibrillation (case 3), mitral valvular disease with atrial fibrillation (case 4), old myocardial infarction with atrial fibrillation (case 5), and only atrial fibrillation (case 6). Complete occlusion of the ipsilateral proximal internal carotid artery was found in five patients on cervical MR angiograms (cases 3, 5, 7, 9, and 10).

Classification of MR Imaging Patterns

MR angiograms showed cerebral arterial occlusion in 10 patients and normal findings in two patients. CBV maps showed obviously decreased CBV in the affected vascular distribution in eight patients, increased CBV in two patients, and normal CBV in two patients. Therefore, these combined CBV and MR angiographic findings were classified into three patterns as follows: arterial occlusion and decreased CBV (cases 1–8) (Fig 1); arterial occlusion and increased CBV (cases 9 and 10) (Fig 2); and no arterial occlusion and normal CBV (cases 11 and 12). The mean CBV ratios in these three imaging patterns were 0.19 (range, 0.03–0.36), 1.20 (range, 1.17–1.23), and 1.00 (range, 0.98–1.01), respectively, and were statistically significantly different ($P = .021$ by Kruskal-Wallis test).

Time–signal intensity curves showed no reduction of signal intensity in the region of decreased CBV in any of the eight patients with the pattern of arterial occlusion and decreased CBV (Fig 1E). In two patients with the pattern of arterial occlusion and increased CBV, delayed arrival time and delayed washout of the contrast material in the region of increased CBV was observed, suggesting recruitment of blood flow through collaterals (Fig 2E). In two patients with the pattern of no arterial occlusion and normal CBV, there were no differences in signal reduction, arrival time, or washout pattern of the contrast material between the hemispheres.

Comparison of CBF Ratios on SPECT

Brain SPECT was performed in nine of 12 patients. The mean CBF ratios measured on SPECT were 0.39 (range, 0.20–0.65) in six patients with the pattern of arterial occlusion and decreased CBV (Fig 1F), 0.85 (range, 0.81–0.89) in two patients with the pattern of arterial occlusion and increased CBV (Fig 2F), and 0.99 in one patient with the pattern of no arterial occlusion and normal CBV. Although CBF ratios in these three imaging patterns were obviously different, there was no statistically significant difference, owing to the small

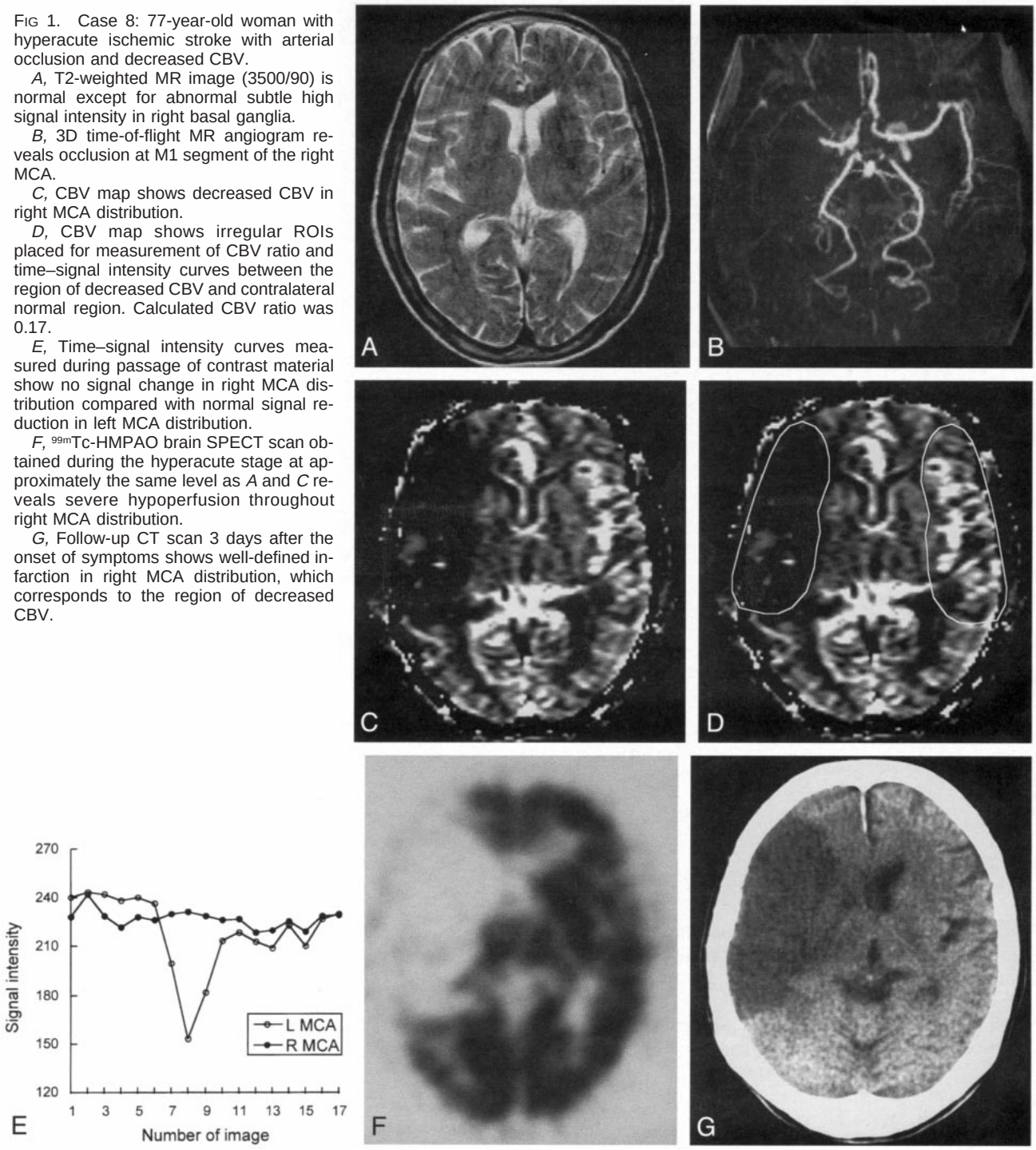

FIG 1. Case 8: 77-year-old woman with hyperacute ischemic stroke with arterial occlusion and decreased CBV.

A, T2-weighted MR image (3500/90) is normal except for abnormal subtle high signal intensity in right basal ganglia.

B, 3D time-of-flight MR angiogram reveals occlusion at M1 segment of the right MCA.

C, CBV map shows decreased CBV in right MCA distribution.

D, CBV map shows irregular ROIs placed for measurement of CBV ratio and time–signal intensity curves between the region of decreased CBV and contralateral normal region. Calculated CBV ratio was 0.17.

E, Time–signal intensity curves measured during passage of contrast material show no signal change in right MCA distribution compared with normal signal reduction in left MCA distribution.

F, ^{99m}Tc-HMPAO brain SPECT scan obtained during the hyperacute stage at approximately the same level as *A* and *C* reveals severe hypoperfusion throughout right MCA distribution.

G, Follow-up CT scan 3 days after the onset of symptoms shows well-defined infarction in right MCA distribution, which corresponds to the region of decreased CBV.

number of patients ($P = .061$ by Kruskal-Wallis test).

Comparison of Short-Term Outcomes

Neurologic deficits of eight patients with the pattern of arterial occlusion and decreased CBV were not significantly changed at 24 hours after symptom onset, even though slightly improved in one patient (case 6) and slightly worse in one patient (case 8). Interval changes in the NIH Stroke Scale score between the hyperacute stage and 24 hours after symptom onset were not statistically significant in this imaging pattern ($P = .35$ by Wilcoxon matched-pairs signed rank test). Neurologic deficits in all four patients with the remaining two imaging patterns were completely resolved at 24 hours after symptom onset; however, the Wilcoxon matched-pairs signed rank test failed to reveal a statistical significance in interval changes in the NIH Stroke Scale score, probably owing to the small number of patients ($P = .068$).

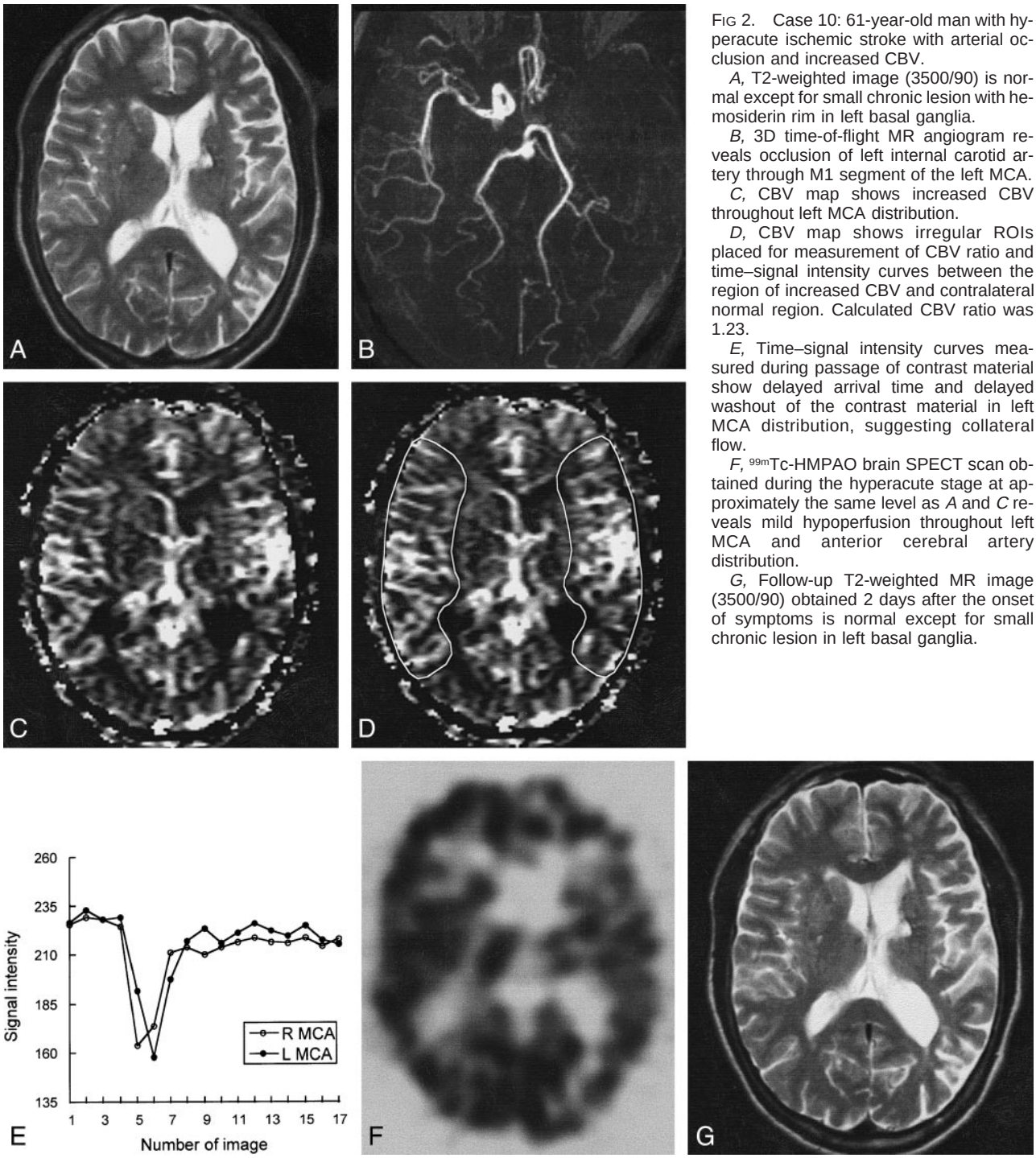

FIG 2. Case 10: 61-year-old man with hyperacute ischemic stroke with arterial occlusion and increased CBV.

A, T2-weighted image (3500/90) is normal except for small chronic lesion with hemosiderin rim in left basal ganglia.

B, 3D time-of-flight MR angiogram reveals occlusion of left internal carotid artery through M1 segment of the left MCA.

C, CBV map shows increased CBV throughout left MCA distribution.

D, CBV map shows irregular ROIs placed for measurement of CBV ratio and time–signal intensity curves between the region of increased CBV and contralateral normal region. Calculated CBV ratio was 1.23.

E, Time–signal intensity curves measured during passage of contrast material show delayed arrival time and delayed washout of the contrast material in left MCA distribution, suggesting collateral flow.

F, ^{99m}Tc-HMPAO brain SPECT scan obtained during the hyperacute stage at approximately the same level as *A* and *C* reveals mild hypoperfusion throughout left MCA and anterior cerebral artery distribution.

G, Follow-up T2-weighted MR image (3500/90) obtained 2 days after the onset of symptoms is normal except for small chronic lesion in left basal ganglia.

Comparison of Development of Infarction

Follow-up CT or MR examinations in all eight patients with the pattern of arterial occlusion and decreased CBV showed infarctions, whose extent correlated well with the region of CBV and CBF abnormalities (Fig 1G). In two patients with the pattern of arterial occlusion and increased CBV, infarctions did not develop on initial follow-up images (Fig 2G). The development of infarctions was statistically significantly different between these two patterns ($P = .022$ by Fisher's exact test). In one patient (case 9), however, watershed infarction developed in the cerebral deep white matter 3 days after the first follow-up study. In two patients with the pattern of no arterial occlusion and normal CBV, follow-up imaging was not performed.

Discussion

Aggressive thrombolytic therapy has been performed in patients with acute ischemic stroke to restore blood flow and to keep the potentially sal-

vageable penumbral tissue surrounding an infarcted core from progressing to infarction. To increase the efficacy and reduce the complication of thrombolytic therapy, patients should be diagnosed promptly and treated within the first few hours after the onset of symptoms. Although there are various subtypes of acute ischemic stroke (1), comprehensive determination of the origin and pathophysiology of an individual stroke is not easy during the limited therapeutic window that is available. Regardless of the origin of thromboembolic vascular occlusion, however, abrupt major arterial occlusion leading to vascular compromise may be treatable by thrombolytic therapy. Other subtypes of acute ischemic stroke, such as slowly progressive chronic arterial occlusion, small arterial occlusion, and early reperfusion of the occluded artery, may require other types of treatment.

In this study, we evaluated the hemodynamic status of the ischemic brain on a conventional MR imaging system by using perfusion-weighted MR imaging along with MR angiography. These techniques can provide dynamic perfusion information on the tissue level and static morphologic information about the large arteries, respectively. We classified the combined perfusion-weighted MR imaging and MR angiographic findings in hyperacute ischemic stroke into three patterns: arterial occlusion and decreased CBV, arterial occlusion and increased CBV, and no arterial occlusion and normal CBV. Because these imaging patterns were associated with different short-term clinical outcomes, they reflect different clinical subtypes of hyperacute ischemic stroke, each with a different hemodynamic status.

Although these imaging patterns are not based on the origin or pathophysiology of stroke, we speculate that each corresponds to a distinct clinical subtype: the pattern of arterial occlusion and decreased CBV suggests abrupt arterial occlusion leading to ongoing infarction; the pattern of arterial occlusion and increased CBV suggests slowly progressive chronic arterial occlusion, giving collaterals the chance to develop and causing ischemia without ongoing infarction but with the risk of future stroke; and the pattern of no arterial occlusion and normal CBV suggests small arterial occlusion or early reperfusion of the occluded artery. This classification of MR imaging patterns may, therefore, have an impact on the type of treatment appropriate for each clinical subtype. Thrombolytic therapy could be beneficial for abrupt arterial occlusion leading to ongoing infarction (2–5). For slowly progressive chronic arterial occlusion with relatively well-developed collaterals, anastomotic bypass surgery or endarterectomy may be preferred (14). For small arterial occlusion or early reperfusion of the occluded artery, long-term medical antithrombotic therapy may be recommended (15).

CBV is a hemodynamic parameter that can easily be calculated from dynamic T2*-weighted MR imaging data. CBV correlates positively with CBF in the normal condition (16). When severe vascular compromise occurs, such as with abrupt arterial occlusion, CBV falls immediately with CBF, and infarction develops thereafter (17–19). Of our eight patients with the pattern of arterial occlusion and decreased CBV, the six who underwent SPECT also showed markedly decreased CBF in the same regions as on the CBV maps, and all patients had large infarctions on follow-up images in the region of decreased CBV. Five of these patients had a cardiac embolic source, suggesting abrupt embolic occlusion. A question may be raised about the reversibility of tissue injury in the region of decreased CBV. As yet, there have been few MR studies appraising this issue. Kluytmans et al (12) reported that the size of the final infarction was best predicted by CBV and CBF maps, suggesting that the region of decreased CBV was already damaged irreversibly. However, those patients were examined a rather long time after symptom onset (mean, 24 hours; range, 2.5–45 hours). Copen et al (11), reporting on patients examined within 10 hours after symptom onset, found that the size of the final infarction was larger than the CBV abnormality and smaller than the CBF abnormality. On the basis of these two studies, we can speculate that the decreased CBV at the acute stage may reflect irreversible damage and may grow over time, even after 10 hours from symptom onset. The therapeutic window still remains a point of debate; the frequency of complications is the major concern (20). The consensus is that 6 hours after symptom onset is the maximum time before treatment should be initiated, although the earlier the better (21).

When arterial occlusion occurs slowly, giving collaterals a chance to develop, CBV increases by compensatory vasodilatation subsequent to reduction of CBF (22–24). In this ischemic condition, tissues are viable but may be insufficiently perfused (ie, misery perfusion), depending on the degree of collateral development, and may be at risk for infarction (9, 25). This relationship between CBF and CBV was demonstrated in two patients with the pattern of arterial occlusion and increased CBV in this study who had slightly decreased CBF but slightly increased CBV. Both patients showed delayed arrival and washout of contrast material on the time–signal intensity curves, suggesting a recruitment of blood flow via collaterals. In one of these patients, however, watershed infarction developed in the cerebral deep white matter 3 days after the first follow-up imaging study. Temporary hypoperfusion caused by hypotension or dehydration may induce stroke symptoms in this clinical subtype. Patients with this clinical subtype tend to have a higher prevalence of prior transient ischemic attacks and/or relatively lower NIH Stroke Scale scores than do patients with other clinical subtypes.

Absence of arterial occlusion and normal CBV are associated with better prognosis in acute ischemic stroke (6, 19, 26), although early recanalization of vascular obstruction after development of

irreversible ischemic damage may occur occasionally, even within a few hours after the onset of symptoms (27, 28). Therefore, normal angiographic findings and CBV at the hyperacute stage, as observed in two patients in this study, suggest early reperfusion of an occluded artery or small arterial occlusion that cannot be depicted by MR imaging.

Although the three stroke subtypes we propose can be differentiated clinically and radiologically several days after the onset of symptoms, identifying them within the short therapeutic window at the hyperacute stage is not easy with clinical examination and conventional CT and/or MR imaging alone. Therefore, the combination of perfusion-weighted MR imaging and MR angiography, which can be performed on a conventional MR imaging system, may be useful in subclassifying hyperacute ischemic stroke and, consequently, in guiding the choice of treatment for each subtype.

Perfusion-weighted MR imaging and ^{99m}Tc-HMPAO SPECT reflect simply the current perfusion status, and cannot provide information about tissue viability. Therefore, CBF and CBV measurement alone cannot differentiate irreversible tissue damage from salvageable tissue. Two previous SPECT studies suggest a lesion-to-contralateral CBF ratio of 0.39 to 0.48 (29) and 0.6 (27), respectively, as thresholds to distinguish infarcted from viable tissue. The mean lesion-to-contralateral CBF ratio of 0.39 (range, 0.20–0.65) in this study is similar to the results of these previous studies. To our knowledge, there has been no MR study to investigate the CBV threshold for the development of infarction. The mean lesion-to-contralateral CBV ratio of 0.19 (range, 0.03–0.36) in our study may suggest a viability threshold when there is a decrease of CBF and CBV after acute arterial occlusion. Although the present study showed obviously different CBF and CBV data between patients with and without ongoing infarction, determination of CBF and CBV thresholds for development of infarction requires further investigation with a standardized methodology.

This study has several technical limitations. First, diffusion-weighted imaging could not be performed in our imaging protocol because we used a conventional MR imaging system that was not equipped with sufficiently strong and fast gradients. Diffusion-weighted MR imaging can play an additional important role in guiding the treatment of hyperacute ischemic stroke and in helping to differentiate the clinical subtypes by depicting the early ischemic damage of the tissue, which cannot be directly evaluated on perfusion-weighted MR images. The second limitation is that only a single section can be evaluated with our dynamic contrast-enhanced T2*-weighted imaging technique. Thus, concerns may be raised about the reliability of data obtained at a single section without covering the whole region of cerebral infarction. The third limitation is the low temporal resolution, which provides only a few data points useful for tracking the first pass of contrast material. Therefore, we did not calculate other hemodynamic parameters (ie, CBF and mean transit time), because these parameters depend on temporal resolution more than does CBV. All these limitations could be mitigated with the use of an echo-planar imaging technique, with its superior temporal resolution and diffusion-weighted imaging capability.

Conclusion

In a small group of patients in this study, the combined perfusion-weighted MR imaging and MR angiographic findings in hyperacute ischemic stroke were classified into three imaging patterns with different clinical outcomes: arterial occlusion and decreased CBV, arterial occlusion and increased CBV, and no arterial occlusion and normal CBV. Although these imaging patterns are not classified by origin or pathophysiology of stroke, we speculate that each pattern corresponds to distinct clinical subtypes with different clinical outcomes. Consequently, we think that the combined use of perfusion-weighted MR imaging and MR angiography in hyperacute ischemic stroke, even on a conventional MR imaging system, can differentiate various patterns of hemodynamic status, and may play a substantial role in guiding the choice of treatment.

References

1. Mohr JP, Sacco RL. **Classification of ischemic stroke.** In: Barnett HJM, Mohr JP, Stein BM, Yatsu FM, eds. *Stroke Pathophysiology, Diagnosis and Management.* 2nd ed. New York: Churchill Livingstone; 1992;271–283
2. Barr JD, Mathis JM, Wildenhain SL, Wechsler L, Jungreis CA, Horton JA. **Acute stroke intervention with intraarterial urokinase infusion.** *J Vasc Interv Radiol* 1994;5:705–713
3. Barnwell SL, Clark WM, Nguyen TT, O'Neill OR, Wynn ML, Coull BM. **Safety and efficacy of delayed intracranial urokinase therapy with mechanical clot disruption for thromboembolic stroke.** *AJNR Am J Neuroradiol* 1994;15:1817–1822
4. Barnwell SL, Nesbit GM, Clark WM. **Local thrombolytic therapy for cerebrovascular disease: current Oregon Health Sciences University experience (July 1991 through April 1995).** *J Vasc Interv Radiol* 1995;6:78S–82S
5. del Zoppo GJ, Higashida RT, Furlan AJ, Pessin MS, Rowley HA, Gent M. **PROACT: a phase II randomized trial of recombinant pro-urokinase by direct arterial delivery in acute middle cerebral artery stroke. PROACT investigators: prolyse in acute cerebral thromboembolism.** *Stroke* 1998;29:4–11
6. Sorensen AG, Buonanno FS, Gonzalez RG, et al. **Hyperacute stroke: evaluation with combined multisection diffusion-weighted and hemodynamically weighted echo-planar MR imaging.** *Radiology* 1996;199:391–401
7. Barber PA, Darby DG, Desmond PM, et al. **Prediction of stroke outcome with echoplanar perfusion- and diffusion-weighted MRI.** *Neurology* 1988;51:418–426
8. Sunshine JL, Lewin JS, Tarr RW, Lanzieri CF, Landis DMD, Selman WR. **Echo-planar perfusion and diffusion imaging in acute stroke therapy.** In: *Proceedings on CD-ROM: International Society for Magnetic Resonance in Medicine 1998.* Sidney: International Society for Magnetic Resonance in Medicine; 1998:1150
9. Reith W, Heiland S, Erb G, Benner T, Forsting M, Sartor K. **Dynamic contrast-enhanced T2*-weighted MRI in patients with cerebrovascular disease.** *Neuroradiology* 1997;39:250–257
10. Kim JH, Shin T, Chung JD, et al. **Temporal pattern of blood volume change in cerebral infarction: evaluation with dynamic contrast-enhanced T2*-weighted MR imaging.** *AJR Am J Roentgenol* 1998;170:765–770

11. Copen WA, Koroshetz WJ, Ostergaard L, et al. **Prediction of ischemic injury in acute human stroke with diffusion- and perfusion-weighted MRI.** In: *Proceedings on CD-ROM: International Society for Magnetic Resonance in Medicine 1997.* Vancouver: International Society for Magnetic Resonance in Medicine; 1997:272
12. Kluytmans M, van Everdingen KJ, Ramos LMP, Viergever MA, van der Grond J. **Final infarct size prediction by perfusion weighted imaging in patients with an acute cerebral infarction.** In: *Proceedings on CD-ROM: International Society for Magnetic Resonance in Medicine 1998.* Sidney: International Society for Magnetic Resonance in Medicine; 1998:1275
13. Belliveau JW, Rosen BR, Kantor HL, et al. **Functional cerebral imaging by susceptibility-contrast NMR.** *Magn Reson Med* 1990;14:538–546
14. Robertson JT, Barnett HJM. **Surgery for symptomatic disease due to arteriosclerosis of the carotid artery.** In: Barnett HJM, Mohr JP, Stein BM, Yatsu FM, eds. *Stroke Pathophysiology, Diagnosis and Management.* 2nd ed. New York: Churchill Livingstone; 1992:1005–1020
15. Barnett HJM. **Antithrombotic therapy in cerebral arterial disease.** In: Barnett HJM, Mohr JP, Stein BM, Yatsu FM, eds. *Stroke Pathophysiology, Diagnosis and Management.* 2nd ed. New York: Churchill Livingstone; 1992:929–941
16. Leenders KL, Perani D, Lammertsma AA, et al. **Cerebral blood flow, blood volume and oxygen utilization: normal values and effect of age.** *Brain* 1990;113:27–47
17. Todd NV, Picozzi P, Crockard HA. **Quantitative measurement of cerebral blood flow and cerebral blood volume after cerebral ischaemia.** *J Cereb Blood Flow Metab* 1986;6:338–341
18. Hamberg LM, Macfarlane R, Tasdemiroglu E, et al. **Measurement of cerebrovascular changes in cats after transient ischemia using dynamic magnetic resonance imaging.** *Stroke* 1993;24:444–451
19. Rother J, Guckel F, Neff W, Schwartz A, Hennerici M. **Assessment of regional cerebral blood volume in acute human stroke by use of single-slice dynamic susceptibility contrast-enhanced magnetic resonance imaging.** *Stroke* 1996;27:1088–1093
20. Beauchamp NJ Jr, Bryan RN. **Acute cerebral ischemic infarction: a pathophysiologic review and radiologic perspective.** *AJR Am J Roentgenol* 1998;171:73–84
21. Endo S, Kuwayama N, Hirashima Y, Akai T, Nishijima M, Takaku A. **Results of urgent thrombolysis in patients with major stroke and atherothrombotic occlusion of the cervical internal carotid artery.** *AJNR Am J Neuroradiol* 1998;19:1169–1175
22. Heiss WD, Herholz K. **Assessment of pathophysiology of stroke by positron emission tomography.** *Eur J Nucl Med* 1994;21: 455–465
23. Powers WJ, Grubb RL, Raichle ME. **Physiological responses to focal cerebral ischemia in humans.** *Ann Neurol* 1984;16:546–552
24. Sabatini U, Celsis P, Viallard G, Rascol A, Marc-Vergnes J-P. **Quantitative assessment of cerebral blood volume by single-photon emission computed tomography.** *Stroke* 1992;22:324–330
25. Mohr JP, Gautier JC, Pessin MS. **Internal carotid artery disease.** In: Barnett HJM, Mohr JP, Stein BM, Yatsu FM, eds. *Stroke Pathophysiology, Diagnosis and Management.* 2nd ed. New York: Churchill Livingstone; 1992;285–335
26. Wardlaw JM, Dennis MS, Lindley RI, Warlow CP, Sandercock PAG, Sellar R. **Does early reperfusion of a cerebral infarct influence swelling in the acute stage or the initial clinical outcome?** *Cerebrovasc Dis* 1993;3:86–93
27. Shimosegawa E, Hatazawa J, Inugami A, et al. **Cerebral infarction within six hours of onset: prediction of completed infarction with technetium-^{99m}-HMPAO SPECT.** *J Nucl Med* 1994; 35:1097–1103
28. Shintani S, Tsuruoka S, Yasuhiro S. **Spurious hyperfixation of hexamethylpropyleneamine oxime in acute embolic stroke.** *AJNR Am J Neuroradiol* 1995;16:1532–1535
29. Nakano S, Kinoshita K, Jinnouchi S, Hoshi H, Watanabe K. **Critical cerebral blood flow thresholds studied by SPECT using xenon-133 and iodine-123 iodoamphetamine.** *J Nucl Med* 1989; 30:337–342